

ADP-ribose polymer depletion leads to nuclear Ctf re-localization and chromatin rearrangement

Tiziana Guastafierro^{*,†,¶}, Angela Catizone^{‡,¶}, Roberta Calabrese^{*,†}, Michele Zampieri^{*,†}, Oliviano Martella[§], Maria Giulia Bacalini^{*,†}, Anna Reale^{*,†}, Maria Di Girolamo[§], Margherita Micheli^{*}, Dawn Farrar^{||}, Elena Klenova^{||}, Fabio Ciccarone^{*,†} and Paola Caiafa^{*,†}.

^{*}Department of Cellular Biotechnologies and Haematology “Sapienza” University Rome, V.le Regina Elena 324, 00161 Rome, Italy,

[†]Pasteur Institute-Fondazione Cenci Bolognetti, P.le A. Moro 5, 00185 Rome, Italy,

[‡]Department of Anatomy, Histology, Forensic Medicine and Orthopedics, Section of Histology and Embryology, Faculty of Pharmacy and Medicine, “Sapienza” University Rome, V.le Regina Elena 324, 00161 Rome, Italy,

[§]Consorzio Mario Negri Sud, Via Nazionale 8/A, 66030 Santa Maria Imbaro, Chieti Italy

^{||}Department of Biological Sciences, University of Essex, Wivenhoe Park, Colchester, Essex CO4 3SQ, United Kingdom

[¶]Both authors contributed equally to this work.

Short Title: Ctf nuclear re-localization PAR depletion-dependent

Corresponding authors:

Prof. Paola Caiafa,
Dept of Cellular Biotechnologies and Haematology “Sapienza” University, 7 via Chieti,
00161, Rome, Italy
Tel.: 0039 0649976530;
Fax: 0039 0644231961;
E-mail: caiafa@bce.uniroma1.it

Dr. Fabio Ciccarone
Dept of Cellular Biotechnologies and Haematology “Sapienza” University
7, via Chieti, 00161
Rome, Italy
Tel.: 0039 0649976556,
Fax: 0039 0644231961,
E-mail: ciccarone@bce.uniroma1.it

Number of Words: 4627

SYNOPSIS

CCCTC binding factor (Ctcf) directly induces poly(ADP-ribose)polymerase-1 (Parp1) activity and its poly(ADP-ribosyl)ation (PARylation) in absence of DNA damage. Ctcf, in turn, is substrate for this post-synthetic modification and as such it is covalently and non-covalently modified by ADP-ribose polymers (PARs). Moreover, PARylation is able to protect from DNA methylation certain DNA regions bound by Ctcf. We recently reported that de novo methylation of Ctcf target sequences due to overexpression of poly(ADP-ribose)glycohydrolase (PARG) induces loss of Ctcf binding. Considering this, here we investigate to what extent PARP activity is able to affect nuclear distribution of Ctcf. Notably, Ctcf lost its diffuse nuclear localization following PAR depletion and accumulated at the periphery of the nucleus where it linked with nuclear pore complex proteins remaining external to the perinuclear Lamin B1 ring. We demonstrated that PAR depletion-dependent perinuclear localization of Ctcf was due to its blockage from entering the nucleus. Besides Ctcf nuclear delocalization, the outcome of PAR depletion led to changes in chromatin architecture. Immunofluorescence analyses indicated DNA re-distribution, a generalized genomic hypermethylation and an increase of inactive vs active chromatin marks in PARG overexpressing or Ctcf silenced cells. Together these data underline the importance of the crosstalk between Parp1 and Ctcf in the maintaining of nuclear organization.

Key words: PARylation, chromatin structure, Ctcf, Parg, Parp1

Abbreviation Footnote

ADP-ribose polymers, PAR; antibody, Ab; CCCT binding factor, Ctcf; Confocal Laser Scanner, CLSM; dimethyl-Histone H3 (Lys4), 2me-H3K4; DNA 5-methylcytosine, 5-MeCyt; Endoplasmic Reticulum, ER; nuclear pore complex, NPC; Poly(ADP-ribose) glycohydrolase, PARG; Poly(ADP-ribosyl)ation, PARylation; Poly(ADP-ribosyl)polymerase, PARP; trimethyl-Histone H3 (Lys9), 3me-H3K9.

INTRODUCTION

Poly(ADP-ribosyl)ation (PARylation), a post-translational modification catalyzed by enzymes of the poly(ADP-ribose) polymerase (PARP) family, leads to the covalent introduction of the ADP-ribose units onto acceptor proteins and also onto PARPs themselves [1]. Poly(ADP-ribose) glycohydrolase (PARG) degrades ADP-ribose polymers (PARs) reversing the modification by its exo and endoglycosydase activities [2]. PARs, present on covalently PARylated proteins are able to interact non-covalently with other proteins binding a 20-amino-acid PAR-binding motif [3], as well as the PAR-binding zinc finger (PBZ) motif [4] and the well-characterized “macro domain” [5]. Parp1 (also termed as ARTD1 based on a recent nomenclature [6]) is the founder of PARP family [1]; in its PARylated form Parp1 participates in the emergency and housekeeping roles being involved in DNA damage repair and in the control of gene expression, respectively.

Parp1 also orchestrates genome organization by regulating genome-wide transcription [7] and epigenetic states of chromatin [8]. In the latter, Parp1 leads to chromatin decondensation PARylating itself as well as core histones and the linker histone H1, while the absence of

PARylation induces chromatin condensation [8, 9]. Chromatin condensation can be mediated by histone macro2A variant, whose non-histone domain (NHD) recruits Parp1 inducing its inhibition [5, 10]. Moreover, Parp1 activity is also involved in counteracting the ATP-dependent nucleosome-remodelling factor ISWI [11] and in inhibiting enzymes involved in chromatin repression such as the histone demethylase KDM5B [9]. PARylation is also important for the maintaining of DNA methylation patterns of the genome. In fact, PARylated Parp1 and DNA methyltransferase 1 (Dnmt1) interact and PARs, present on Parp1 itself, bind non-covalently with Dnmt1 preventing its access to DNA and thus its DNA methyltransferase activity. As a consequence, PAR depletion, induced through the treatment of cells with a competitive inhibitor of PARP activity [12] or through ectopic over-expression of PARG [13], leads to the introduction of new anomalous methyl groups onto unmethylated DNA regions. Concerning genome regions, where non methylated state is necessary for their functions the outcome of the process they control, the presence of PARs on them has been found to be important [13, 14-18]. The multifunctional CCCTC binding factor (Ctcf) has been identified as an important player by which PARylation preserves the unmethylated state of some regulatory DNA sequences [15, 16, 18]. In fact, Ctcf by itself is able to activate PARylation of Parp1 even in the absence of DNA damage [19]. Moreover, Ctcf undergoes covalent [14] and non-covalent PARylation [18] and how Ctcf selects these modifications to perform its numerous functions remains to be defined.

The fact that Ctcf binds selectively non-methylated DNA sequences and that out of the numerous Ctcf-binding sites on genome many of them coincide with those of Parp1 [16], indicates that Ctcf can mark those regions that must be maintained non methylated in the genome. Maintaining of non-methylated states could be reached through the formation of Ctcf-Parp1 complex, PARylation of Parp1 and, in turn, inhibition of Dnmt1 activity [19]. This mechanism has been indicated as the one involved in maintaining non-methylated *p16* gene promoter CpG island [15] and in preserving the methylation profile of the differentially methylated region 1 (*DMR1*) at the *Igf2/H19* imprinted locus [18]. Based on the above, PARylated Parp1, following the binding with Ctcf, would become an epigenetic mark of DNA regions that have to be maintained non methylated in the genome [20]. Considering that DNA hypermethylation dependent on PAR depletion induces the loss of Ctcf binding from DNA regions and that putative target sequences for Ctcf and Parp1 often overlap, the aim of this research is to verify whether Ctcf localization is influenced by PARs.

EXPERIMENTAL

Subcellular fractionation and western blot analysis

Nuclear and cytosolic fractions were collected from trypsinized and phosphate-buffered saline (PBS)-washed cells by centrifugation following incubation (30 min) in isolation buffer containing 10 mM 4-(2-hydroxyethyl)-1-piperazineethanesulfonic acid (HEPES) pH 7.9; 10 mM KCl, 1.5 mM MgCl₂, 50 mM NaF; 0.5 mM Dithiothreitol; 0.3 mM phenylmethylsulfonyl fluoride (PMSF). Nuclear fraction was lysed in RIPA buffer (50 mM Tris-HCl pH 8, 150 mM NaCl, 0.5% sodium deoxycholate, 0.1% SDS, 1% Nonidet P-40, 1 mM EDTA). Both buffers were supplemented with protease inhibitors (complete EDTA-free, Roche Applied Science). Protein concentration was determined using the Bradford protein assay reagent (Bio-Rad) with bovine serum albumin (Promega) as standard. Equal protein amounts were subjected to 8% SDS-PAGE and blotted onto Hybond-ECL nitrocellulose membranes (Amersham Biosciences). The antibodies employed were as follows: mouse

monoclonal Ab anti PAR (10 HA, Trevigen), mouse monoclonal Ab anti Myc (9E10 clone, hybridoma-conditioned medium) [13], mouse monoclonal Ab anti Parp1 (C2-10, Alexis), rabbit polyclonal Ab anti Ctf (Millipore), goat polyclonal Ab anti Ctf (SantaCruz), mouse monoclonal Ab anti α Tubulin (clone B-5-1-2, Sigma Aldrich), rabbit polyclonal Ab anti Lamin B1 (AbCam), mouse monoclonal Ab anti NPC (AbCam), donkey anti goat, goat anti mouse and anti rabbit horseradish peroxidase-conjugated antibodies (Santa Cruz Biotechnology).

Transfection of cells

In transfection experiments 0.7×10^6 cells were seeded in 60×15 mm culture dishes and transfected with Lipofectamine Plus reagent (Invitrogen) adopting the manufacturer's protocol. Assays were performed with $4 \mu\text{g}/\text{dish}$ of purified plasmid DNA of either empty myc-vector (pcs2) as control or Myc-PARG construct (pcs2-Myc-PARG) [13] together with $0.4 \mu\text{g}/\text{dish}$ of pBabe-puro (Addgene) vector for puromycin selection of transfected cells. After 24 hrs cells were incubated for further 72 hrs in culture medium supplemented with puromycin ($2.5 \mu\text{g}/\text{ml}$, Calbiochem). In pcs2-Myc-PARG / EGFP-Ctf or pcs2-Myc-PARG / EGFP-Ctf mutated co-transfection experiments, 1.5×10^5 cells were seeded in 35 mm μ -Dish (ibidi GmbH) and transfected with Lipofectamine Plus reagent (Invitrogen) adopting the manufacturer's protocol.

Knockdown experiments

In experiments of *Ctf*, *Parp1* and *Parp2* silencing, 0.16×10^6 cells were seeded in 60×15 mm culture dishes and transfected for 48hrs with siRNA (Dharmacon) at a final concentration of 50 nM using Lipofectamine 2000 reagent (Invitrogen) following manufacturer's instructions.

Co-immunoprecipitation

Nuclear and cytosol fractions or total L929 cells were lysed in IP buffer (50 mM Tris-HCl pH 7.5, 5 mM EDTA, 300 mM NaCl, 1% Nonidet P-40, 1% Triton X-100) supplemented with protease-inhibitors (complete EDTA-free, Roche Applied Science). Lysates (1.5 mg) were pre-cleared with protein A-agarose beads (Upstate) on a rotative shaker at 4°C for 2 hrs and 30 min. Pre-cleared lysates were incubated with specific antibodies rabbit polyclonal Ab anti Ctf (Millipore) and with normal rabbit IgG (Santa Cruz Biotechnology) on a rotative shaker overnight at 4°C . The agarose beads, previously saturated with bovine serum albumin ($1 \mu\text{g}/\mu\text{l}$) overnight, were added to the lysate/Ab solutions and incubated for 2 hrs on a rotative shaker at 4°C . Subsequently, beads were washed in IP buffer, then boiled in SDS-PAGE sample buffer, and the eluted proteins were analyzed by western blotting.

Confocal and Time-lapse video microscopy

Cells were fixed in paraformaldehyde and permeabilized in 0.2% Triton X-100 in PBS supplemented with 0.5 % BSA for 1 hr at room temperature. Cells were incubated with primary antibody, then washed in PBS and incubated with the secondary antibody. As regards 5-MeCyt staining, cells were permeabilized in PBS, 1% BSA, 0.5% TritonX-100 for 30 min., then washed with PBS and treated with 4 N HCl for 30 min at 37°C . Following extensive PBS washes, cells were blocked in PBS, 1% BSA, 0.1% TritonX-100 for 30 min and incubated with anti 5-MeCyt antibody at 4°C overnight. The cells were then extensively

washed and incubated for 1 hr at RT with the secondary antibodies, and then treated with RNase A (1 mg/ml) for 30 min.

Antibodies employed were the same used in western blot experiments. Other antibodies used were: rabbit polyclonal Ab anti nucleophosmin/B23 (AbCam), mouse monoclonal Ab anti 5-MeCyt (eurogentec), rabbit polyclonal Ab anti 2me-H3K4 (millipore) and rabbit polyclonal Ab anti 3Me-H3K9 (millipore). Cells were stained with TO-PRO-3 (invitrogen) according to the manufacturer's instructions.

Secondary antibodies employed were the following: TRITC conjugated donkey anti rabbit; FITC conjugated donkey anti goat; TRITC conjugated donkey anti mouse (Jackson ImmunoResearch).

For immunolocalization, a Leica confocal microscope (Laser Scanning TCS SP2) equipped with Ar/ArKr and HeNe lasers was utilized. The images were acquired utilizing the Leica confocal software. Laser line was at 488 nm for FITC, 543 nm for TRITC and 633 for TOPRO-3 excitation respectively. The images were scanned under a 40X oil immersion objective. In addition to the qualitative analysis of antigen distribution, a quantitative analysis was carried out using the Leica confocal software. Optical spatial series, each composed of about 15 optical sections with a step size of 1 μ m, were performed. The fluorescence intensity in equivalent sized regions (ROI) was determined by the Leica confocal software [21]. Regarding the time-lapse video experiments, cells were subjected to video microscopy for 24 hours at 37°C.

Generation of the mutant form of pcs2-Myc-PARG overexpression vector

The catalytically inactive Myc-PARG_{E757N} mutant was obtained using the QuickChange site-directed mutagenesis method (Stratagene, La Jolla, CA, USA). The plasmid pcs2-Myc-PARG was used as a template, and the primers for mutagenesis were: PargE757N forw 5'-gcaggactgtgcaagaa**acat**ccgcttttaatcaa-3' and Parg E757N rev 5'-gcggat**gtttt**cttgcaagtcctgcactgg-3' (the mutated nucleotides are in bold). The reaction was performed using the primers at a final concentration of 200 nM, 50 ng of plasmid template, 10 U of Pfu turbo DNA polymerase (Stratagene) and 100 μ M dNTP in 50 μ l of reaction mixture. The reaction conditions were: one step at 95°C for 5 min; 15 cycles at 95°C for 30 s, 55°C for 1 min, 68°C for 1 min, and a final step at 68°C for 7 min. To selectively digest template DNA, the PCR product was treated with DpnI enzyme for 2 hrs at 37 °C and then transformed in TOP10 chemically competent E. coli cells. Clones were sequenced using the primer PargMut seq 5'-gtctgaagtgaagacatcgat-3.

RESULTS

Cellular localization of Ctcf

We first analyzed Ctcf distribution in L929 mouse fibroblasts by Confocal Laser Scanner Microscopy (CLSM). Although Ctcf is located mainly in the nucleoplasm, a clear signal was observed also in the cytoplasm (Fig. 1A, right panel). Quantitative analysis of Ctcf fluorescence in the nucleus and in the cytoplasm at different distances from the nucleus showed a decrease in signal going from the centre to cell periphery. Endogenous Ctcf was diffusely distributed throughout the nucleoplasm while it was undetectable in the nucleoli [22] (Supplementary Fig. 1). Ctcf knock down was performed in L929 cells to verify the specificity of Ctcf staining in the cytosolic compartment. The CLSM showed a dramatic decrease in the Ctcf signal intensities both in the nucleus and in the cytoplasm (Fig. 1B). In

addition, western blot experiments using total, nuclear and cytosolic cell extracts showed that the Ctcf levels decreased in all the cellular subfractions obtained from the Ctcf silenced cells compared to controls (Fig. 1C). Using Lamin B1 as nuclear marker and α Tubulin as a cytosolic marker the purity of nuclear and cytosolic fractions was confirmed (Fig. 1C). The cytosolic distribution of Ctcf was further characterized by co-staining cells for anti α Tubulin one of the major structural constituents of cytoskeleton. Merge image showed that Ctcf and α Tubulin co-localize in the cytosol of L929 cells (Fig 1D). Moreover, co-immunoprecipitation experiments confirmed that Ctcf and α Tubulin interact in vivo (Fig 1E).

PAR depletion induces Ctcf perinuclear accumulation

To analyse if PARylation can affect Ctcf localization, depletion of the endogenous PARs was achieved by semistable ectopic overexpression of the Myc-tagged PARG enzyme (Myc-PARG), as previously described [13]. After 72 hrs of puromycin selection, cells overexpressing Myc-PARG or the corresponding control vector (pcs2) were stained using anti Ctcf antibody and then subjected to CLSM. Figure 2A and supplementary figure 2A show that PARG overexpression leads to a net change of Ctcf distribution with reduced intranuclear staining and perinuclear accumulation. Quantitative analysis of Ctcf fluorescence recovered in the nucleus of PARG overexpressing cells was about 60% less than in control cells. To confirm that the observed re-localization of Ctcf from the nucleus was due to PAR decrease dependent on PARG activity, we transfected L929 cells with pcs2-Myc-PARG_E757N expression vector which carries a mutation in PARG catalytic site completely abolishing its enzymatic activity. Western blot analysis showed that transfection of Myc-PARG_E757N did not affect PAR levels (Fig. 2B). Accordingly, CLSM using anti Ctcf and anti Myc antibodies showed no relocation of Ctcf in cells overexpressing the mutant form of PARG (Fig. 2C). Immunofluorescence using anti Myc antibodies showed that generated PARG mutant did not show any difference from the WT in its nuclear localization (Fig. 2C and supplementary Fig. 2A).

To identify the member of Parp family involved in the control of Ctcf localization, silencing experiments of Parp1 and Parp2, the two enzymes mainly responsible for PAR synthesis in the nucleus, were performed. Confocal microscopy analysis in Parp1 silenced cells showed a decrement of the nuclear level of Ctcf of about 30% (Supplementary Fig. 2B). Differently, silencing of Parp2 does not seem to affect Ctcf localization (Supplementary Fig. 2C). These data were confirmed in fibroblast cells from Parp1 knock out mouse (A1 cells) where the nuclear level of Ctcf was 75% less than Parp1 proficient cells (Supplementary Fig. 2D).

Time-lapse experiments, carried out by co-transfecting cells with pcs2-Myc-PARG and EGFP-CTCF wild type, confirmed that PARG overexpression affects Ctcf localization showing that EGFP-CTCF is not able to enter the nucleus (Figure 2D freezes the movie at 16 hrs post transfection).

To investigate if perinuclear localization of Ctcf dependent on PAR depletion was due to hindrance to enter the nucleus or to its difficulty to be retained within it, we treated cells with an inhibitor of exportin CRM1, Leptomycin B (LMB). However, no difference in Ctcf perinuclear distribution was observed in cells co-transfected with pcs2-Myc-PARG and EGFP-CTCF and treated with LMB (unpublished data). Therefore, it is likely that Ctcf perinuclear accumulation was linked to the hindrance preventing Ctcf from entering the nucleus.

To assess the effect of covalent PARylation on Ctcf nuclear distribution, L929 cells were co-transfected with both pcs2-Myc-PARG and EGFP-CTCF mutant deficient for PARylation [16]. As shown in Figure 2E, the mutated Ctcf is still present in the nucleus of cells in which

PARylation was unaffected (Fig. 2E, frame 1 and 3), while it relocalized at nuclear periphery after PAR depletion (frame 2 and 4) suggesting that covalent PARylation of Ctcf does not play a role in the maintaining of its nuclear localization, which is in agreement with the previous report [16].

Ctcf accumulates out of the Lamin ring

To investigate the effect of PAR depletion on Ctcf nuclear re-localization to the nuclear periphery in more detail, Myc-PARG transfected cells were co-stained with the anti Ctcf and anti Lamin B1 antibodies. As shown in Figure 3A Ctcf accumulates out of the Lamin ring upon PARG overexpression; co-immunoprecipitation experiments revealed the absence of interaction between Ctcf and Lamin B1 (unpublished data). Notably, specific co-immunoprecipitation between Ctcf and proteins of nuclear pore complex (NPC) was observed only in L929 overexpressing PARG (Fig 3B), therefore it is likely that there is interaction between Ctcf and these proteins in vivo.

PARG overexpression induces redistribution of genomic DNA at the nuclear periphery

Previous reports demonstrated that removal of Ctcf from its DNA binding sites leads to the silencing of some Ctcf-target genes by DNA methylation [23, 24]. Furthermore, we demonstrated that such Ctcf removal occurs following PAR depletion [18]. Based on this evidence we hypothesized that the depletion of nuclear Ctcf in PARG overexpressing cells was associated with chromatin rearrangements towards repressive configurations. We analyzed chromatin *status* in three different ways using immunofluorescence experiments: *a*) studying DNA distribution by nuclear staining with TO-PRO-3 (Fig. 4A); *b*) analyzing DNA 5-methylcytosine (5-MeCyt) levels using the anti 5-MeCyt antibodies; *c*) measuring levels of dimethyl-Histone H3 (Lys4) (2me-H3K4) and of trimethyl-Histone H3 (Lys9) (3me-H3K9) as marks of active/inactive chromatin regions, respectively (Fig. 4B).

The distribution of chromatin in *pcs2*-Myc-PARG and control cells was evaluated by means of confocal microscopy using the Leica confocal software to determine the fluorescence intensity of TO-PRO-3 in equivalent sized regions. This analysis was carried out considering approximately 50 optical sections recovered in different spatial series in both samples. Figure 4A shows a representative stack profile of 10 regions of interest (ROI) randomly drawn along the nuclei both in control and Myc-PARG overexpressing cells. The groups of peaks of the figures represent the fluorescence intensity detected by the confocal microscope from the beginning to the end of the sample that is in the total thickness of the examined nuclei.

The image analysis revealed that the position of the maximal amplitude of fluorescence is differently localized in the two samples. In control cells the mean of the value was located at approximately -10,91 μm from the beginning of the sections whereas in the Myc-PARG overexpressing cells the mean was located at approximately -12.54 μm .

This finding suggested that chromatin is mainly located at the periphery region of nuclei in Myc-PARG overexpressing cells.

Investigation of changes in genome methylation levels confirmed our previous data [13] showing that the level of 5-MeCyt dramatically increases in PAR depleted cells (Fig. 4B). At the same time, immunofluorescence analysis using antibodies anti 2me-H3K4 and anti 3me-H3K9 demonstrated a strong increase of condensed *vs* decondensed chromatin structure in Myc-PARG overexpressing cells (Fig. 4B).

Ctcf knocking down experiments were performed to evaluate Ctcf involvement in the maintaining of the proper chromatin arrangement. Similar to the observations made under

PAR depletion conditions, levels of 2me-H3K4 considerably decreased, whereas levels of 5-MeCyt and 3me-H3K9 increased dramatically (Fig. 4C).

DISCUSSION

Genome-wide studies have indicated the presence of thousands of Ctf binding sites [25, 26]. Ctf, by mediating long-range chromatin interactions, does not only play an important role in the organization of chromatin architecture but also in the regulation of gene expression. By bringing the ends of DNA loops together, Ctf defines distinct chromatin domains; their transcriptional activity depends on whether, where and how different types of methylated histones, RNA Pol II and p300 localize on them [27, 28]. Ctf acts both as enhancer blocker and barrier insulator [29]. In the first mechanism, it leads to gene silencing or activation, preventing or driving contacts between enhancer and promoter, respectively [30, 31]. As a barrier insulator, Ctf is able to insulate chromatin regions preventing the diffusion of their active/inactive states into neighbouring chromatin regions [30, 31]. Ctf is multifunctional as seen in its ability to participate in diverse important biological events and this versatility can be explained by specific structural features of Ctf. The eleven Zn-fingers present in the Ctf central domain are responsible for recognizing numerous DNA sequences [32], while all domains are involved in the important interactions with protein partners [33, 34] and undergo post translational modifications [35]. In particular, covalent PARylation occurs within the N-terminal domain [14]. Among the Ctf binding partners, the interaction of the cohesin subunit SA2 with the C-terminal tail of Ctf is involved in important Ctf functions [36]. This protein complex acts at *Igf2/H19 locus*, where epigenetic modifications also play an important role in the control of imprinting. Ctf generally binds unmethylated target sequences [29, 37] and PARP activity may be essential for the maintaining of the correct Ctf regulation. Recent data have evidenced that the presence of PARylated Parp1 is necessary for the expression of some genes controlled by Ctf [13-18] and that DNA methylation due to the absence of PARylation leads to removal of Ctf from DNA [15, 18].

Ctf has been generally described as a nuclear protein. The nuclear Ctf has been reported to associate with both chromosomal arms and centrosomes in metaphase [38], while its distribution is relatively uniform in interphase, with binding sites described to the periphery of nucleolus [39] and to the proximity of matrix [40]. Here we show that Ctf is also detectable in extra-nuclear cell compartments as recently reported by other groups [41]. The specificity of the cytosolic staining of Ctf was confirmed in Ctf-silenced cells showing a decrease of fluorescence in both nucleus and cytosol. Furthermore, the cytosolic localization of Ctf was confirmed by specific co-immunoprecipitation experiments with α Tubulin performed in purified cytosolic fraction.

PAR depletion leads to a loss of the diffuse presence of Ctf within the nucleus with about a 60% reduction and evident re-distribution at its periphery. Specifically, Ctf localizes outside the Lamin ring and immunoprecipitation experiments showed that it was interacting with proteins of nuclear pores only after PAR depletion. Despite the fact that PARs are needed to retain Ctf in the nucleus, the covalent Ctf PARylation does not affect its localization [16], indeed the Ctf mutant deficient for PARylation [16] shows a nuclear diffuse localization similar to that of the wild type protein. In both cases, re-localization to the nuclear periphery takes place following PAR depletion. The possibility remains that the non-covalent interactions between PARs and Ctf play a role in the maintenance of the nuclear localization of Ctf; indeed it is well known that Ctf is able to link very strongly and non-covalently both Parp1-associated and protein-free PARs [18].

Our data indicate that PARylation is pivotal for maintaining nuclear functions of Ctf. Notably Ctf null mice phenotype is lethal [42], while knockout of *Parp1* is predominantly normal [43]. In agreement, our data show that PARG overexpression is more effective than *Parp1* knock-down experiments. This indicates that the control of Ctf nuclear localization PARylation-mediated could be only partially ascribed to *Parp1* which might be replaced by other member of PARP family in its absence.

The finding that in the absence of PARs Ctf loses its intranuclear localization provides an interesting parallel with the data showing that PARylation regulates the intra-nuclear trafficking of important proteins such as p53 and the nuclear factor kappa B (NF- κ B) [44, 45]. In both cases the presence of PARs on proteins prevents and blocks their interaction with the CRM1 exportin and thus the nuclear export [45].

Our results indicate that nuclear localization of Ctf, even if dependent on PAR level, does not share the molecular mechanism described above. These data and the time-lapse analysis support the hypothesis that under condition of PAR depletion, the re-localization of Ctf to the nuclear periphery was due to its difficulty to enter the nucleus, instead of the activation of its export from the nucleus.

Altogether our data demonstrate that PAR levels regulate Ctf cellular distribution, it remains to be defined how decreasing levels of PAR induce Ctf perinuclear re-localization. The nuclear export of Ctf can be mediated by an export system different from the CRM1 and yet to be identified. Alternatively, the import system can be affected, as suggested by our experiments showing that Ctf can interact with NPC, but it cannot pass through the nuclear pore to enter the nucleus. We have recently provided evidence of a close link between ADP-ribosylation and intracellular trafficking [46]. Karyopherin- β 1/importin- β 1 (Kap β 1), which plays a key role in the shuttling of proteins between the cytosol and the nucleus through the NPC, is ADP-ribosylated by the Endoplasmic Reticulum (ER) resident ADP-ribosyltransferase ARTD15 [46]. Future work will clarify the protein(s) and the mechanism(s) involved in the nuclear entry of Ctf.

Recently, perinuclear localization of Ctf has been observed as dependent on ER stress in mouse medulloblastoma cell lines [47]. On this regard, the lack of nuclear PARylation could induce Ctf cellular re-localization ER stress-dependent.

As Ctf and PARylation cooperate in the maintenance of the unmethylated Ctf target sequences, we verified whether and how PAR depletion or Ctf silencing affect chromatin structure. As expected, both conditions lead to the introduction of epigenetic marks typical of condensed/inactive chromatin structure: the genome becomes more methylated [48] and we observed that 2me-H3K4 is less abundant in PAR depleted cells than in control cells while the nuclear level of 3me-H3K9 increases. Analysis carried out to verify possible changes in DNA distribution within nucleus also showed the rearrangement of the genome. The intensity of fluorescence signal recovered in cells where DNA had been stained with TO-PRO-3 DNA shifts to proximity of the nuclear periphery in PAR depleted cells.

These data are in agreement with our previous evidence showing that defective PARylation leads to anomalous hypermethylation of CpG-rich DNA regions [20]. As Ctf is essential for protecting certain gene domains from DNA methylation, reduced nuclear levels of Ctf in PAR-depleted cells could expose CpG-rich Ctf binding regions to aberrant hypermethylation.

Recent evidences highlight a role for Ctf in the transcriptional control of several key-regulators of cell cycle control and progression, whose expression is frequently altered in tumors generally by promoter hypermethylation. Notably, PARylation is necessary for preserving the methylation profile of the DMR1 upstream *Igf2* [18] and for the transcriptional regulation of the tumor suppressor genes *p16INK4a* [15] and *TP53* [49]. Therefore, we can

speculate that defective PARylation by reducing nuclear level of Ctf may be responsible for aberrant hypermethylation and transcriptional deregulation of Ctf target genes.

Globally, our results together with the considerable co-localization of Parp1 and Ctf in the genome [16] reinforce the importance of the cross-talk between Ctf and PARylation in the maintaining of DNA methylation patterns as well as chromatin organization.

FUNDINGS

This work was supported by grants from International FIRB 2006 (RBIN06E9Z8_003) and from Ministero dell'Istruzione, dell'Università e della Ricerca (PRIN 2008, P.C.), Italy.

DEDICATION

This paper is dedicated to the memory of our wonderful colleague and friend, Dr. Maria Malanga, who recently passed away. Her bright mind and her calmness in dealing with any matter will be forever engraved in our hearts.

REFERENCES

- 1 Ame, J. C., Spenlehauer, C. and de Murcia, G. (2004) The PARP superfamily. *Bioessays*. **26**, 882-893
- 2 Bonicalzi, M. E., Haince, J. F., Droit, A. and Poirier, G. G. (2005) Regulation of poly(ADP-ribose) metabolism by poly(ADP-ribose) glycohydrolase: where and when? *Cell. Mol. Life Sci.* **62**, 739-750
- 3 Naegeli, H. and Althaus, F. R. (1991) Regulation of poly(ADP-ribose) polymerase. Histone-specific adaptations of reaction products. *J. Biol. Chem.* **266**, 10596-10601
- 4 Ahel, I., Ahel, D., Matsusaka, T., Clark, A. J., Pines, J., Boulton, S. J. and West, S. C. (2008) Poly(ADP-ribose)-binding zinc finger motifs in DNA repair/checkpoint proteins. *Nature*. **451**, 81-85
- 5 Karras, G. I., Kustatscher, G., Buhecha, H. R., Allen, M. D., Pugieux, C., Sait, F., Bycroft, M. and Ladurner, A. G. (2005) The macro domain is an ADP-ribose binding module. *EMBO J.* **24**, 1911-1920
- 6 Hottiger, M. O., Hassa, P. O., Luscher, B., Schuler, H. and Koch-Nolte, F. (2010) Toward a unified nomenclature for mammalian ADP-ribosyltransferases. *Trends Biochem. Sci.* **35**, 208-219
- 7 Ogino, H., Nozaki, T., Gunji, A., Maeda, M., Suzuki, H., Ohta, T., Murakami, Y., Nakagama, H., Sugimura, T. and Masutani, M. (2007) Loss of Parp-1 affects gene expression profile in a genome-wide manner in ES cells and liver cells. *BMC Genomics*. **8**, 41
- 8 Krishnakumar R, Kraus WL.(2010) The PARP side of the nucleus: molecular actions, physiological outcomes, and clinical targets. *Mol Cell* **39**, 8-24.9 Krishnakumar, R. and Kraus, W. L. (2010) PARP-1 regulates chromatin structure and transcription through a KDM5B-dependent pathway. *Mol. Cell*. **39**, 736-749
- 10 Nusinow, D. A., Hernandez-Munoz, I., Fazzio, T. G., Shah, G. M., Kraus, W. L. and Panning, B. (2007) Poly(ADP-ribose) polymerase 1 is inhibited by a histone H2A variant, MacroH2A, and contributes to silencing of the inactive X chromosome. *J. Biol. Chem.* **282**, 12851-12859
- 11 Sala, A., La Rocca, G., Burgio, G., Kotova, E., Di Gesu, D., Collesano, M., Ingrassia, A. M., Tulin, A. V. and Corona, D. F. (2008) The nucleosome-remodeling ATPase ISWI is regulated by poly-ADP-ribosylation. *PLoS Biol.* **6**, e252
- 12 Reale, A., Matteis, G. D., Galleazzi, G., Zampieri, M. and Caiafa, P. (2005) Modulation of DNMT1 activity by ADP-ribose polymers. *Oncogene*. **24**, 13-19
- 13 Zampieri, M., Passananti, C., Calabrese, R., Perilli, M., Corbi, N., De Cave, F., Guastafierro, T., Bacalini, M. G., Reale, A., Amicosante, G., Calabrese, L., Zlatanova, J. and Caiafa, P. (2009) Parp1 localizes within the Dnmt1 promoter and protects its unmethylated state by its enzymatic activity. *PLoS ONE*. **4**, e4717
- 14 Yu, W., Ginjala, V., Pant, V., Chernukhin, I., Whitehead, J., Docquier, F., Farrar, D., Tavoosidana, G., Mukhopadhyay, R., Kanduri, C., Oshimura, M., Feinberg, A. P., Lobanenkova, V., Klenova, E. and Ohlsson, R. (2004) Poly(ADP-ribosylation) regulates CTCF-dependent chromatin insulation. *Nat. Genet.* **36**, 1105-1110
- 15 Witcher, M. and Emerson, B. M. (2009) Epigenetic silencing of the p16(INK4a) tumor suppressor is associated with loss of CTCF binding and a chromatin boundary. *Mol. Cell*. **34**, 271-284
- 16 Farrar, D., Rai, S., Chernukhin, I., Jagodic, M., Ito, Y., Yammine, S., Ohlsson, R., Murrell, A. and Klenova, E. (2010) Mutational analysis of the poly(ADP-ribosylation) sites of the transcription factor CTCF provides an insight into the mechanism of its regulation by poly(ADP-ribosylation). *Mol. Cell. Biol.* **30**, 1199-1216

- 17 Nocchi, L., Tomasetti, M., Amati, M., Neuzil, J., Santarelli, L. and Saccucci, F. (2011) Thrombomodulin is silenced in malignant mesothelioma by a poly(ADP-ribose) polymerase-1-mediated epigenetic mechanism. *J. Biol. Chem.* **286**, 19478-19488
- 18 Zampieri, M., Guastafierro, T., Calabrese, R., Ciccarone, F., Bacalini, M. G., Reale, A., Perilli, M., Passananti, C. and Caiafa, P. (2012) ADP-ribose polymers localized on Ctf-Parp1-Dnmt1 complex prevent methylation of Ctf target sites. *Biochem. J.* **441**, 645-652
- 19 Guastafierro, T., Cecchinelli, B., Zampieri, M., Reale, A., Riggio, G., Sthandier, O., Zupi, G., Calabrese, L. and Caiafa, P. (2008) CCCTC-binding factor activates PARP-1 affecting DNA methylation machinery. *J. Biol. Chem.* **283**, 21873-21880
- 20 Caiafa, P., Guastafierro, T. and Zampieri, M. (2008) Epigenetics: poly(ADP-ribosylation) of PARP-1 regulates genomic methylation patterns. *Faseb J.*
- 21 Catizone, A., Ricci, G. and Galdieri, M. (2008) Hepatocyte growth factor modulates Sertoli-Sertoli tight junction dynamics. *J. Cell. Physiol.* **216**, 253-260
- 2622 Torrano, V., Navascues, J., Docquier, F., Zhang, R., Burke, L. J., Chernukhin, I., Farrar, D., Leon, J., Berciano, M. T., Renkawitz, R., Klenova, E., Lafarga, M. and Delgado, M. D. (2006) Targeting of CTCF to the nucleolus inhibits nucleolar transcription through a poly(ADP-ribosylation)-dependent mechanism. *J. Cell Sci.* **119**, 1746-1759
- 23 Davalos-Salas, M., Furlan-Magaril, M., Gonzalez-Buendia, E., Valdes-Quezada, C., Ayala-Ortega, E. and Recillas-Targa, F. (2011) Gain of DNA methylation is enhanced in the absence of CTCF at the human retinoblastoma gene promoter. *BMC Cancer.* **11**, 232
- 24 De La Rosa-Velazquez, I. A., Rincon-Arano, H., Benitez-Bribiesca, L. and Recillas-Targa, F. (2007) Epigenetic regulation of the human retinoblastoma tumor suppressor gene promoter by CTCF. *Cancer Res.* **67**, 2577-2585
- 25 Cuddapah, S., Jothi, R., Schones, D. E., Roh, T. Y., Cui, K. and Zhao, K. (2009) Global analysis of the insulator binding protein CTCF in chromatin barrier regions reveals demarcation of active and repressive domains. *Genome Res.* **19**, 24-32
- 26 Phillips, J. E. and Corces, V. G. (2009) CTCF: master weaver of the genome. *Cell.* **137**, 1194-1211
- 27 Handoko, L., Xu, H., Li, G., Ngan, C. Y., Chew, E., Schnapp, M., Lee, C. W., Ye, C., Ping, J. L., Mulawadi, F., Wong, E., Sheng, J., Zhang, Y., Poh, T., Chan, C. S., Kunarso, G., Shahab, A., Bourque, G., Cacheux-Rataboul, V., Sung, W. K., Ruan, Y. and Wei, C. L. (2011) CTCF-mediated functional chromatin interactome in pluripotent cells. *Nat. Genet.* **43**, 630-638
- 28 Chaumeil, J. and Skok, J. A. (2012) The role of CTCF in regulating V(D)J recombination. *Curr. Opin. Immunol.* **24**, 153-159
- 29 Bell, A. C., West, A. G. and Felsenfeld, G. (2001) Insulators and boundaries: versatile regulatory elements in the eukaryotic. *Science.* **291**, 447-450
- 30 Krivega, I. and Dean, A. (2012) Enhancer and promoter interactions-long distance calls. *Curr. Opin. Genet. Dev.* **22**, 79-85
- 31 Yang, J. and Corces, V. G. (2012) Insulators, long-range interactions, and genome function. *Curr. Opin. Genet. Dev.* **22**, 86-92
- 32 Ohlsson, R., Renkawitz, R. and Lobanenkova, V. (2001) CTCF is a uniquely versatile transcription regulator linked to epigenetics and disease. *Trends Genet.* **17**, 520-527
- 33 El-Kady, A. and Klenova, E. (2005) Regulation of the transcription factor, CTCF, by phosphorylation with protein kinase CK2. *FEBS Lett.* **579**, 1424-1434
- 34 Klenova, E. M., Chernukhin, I. V., El-Kady, A., Lee, R. E., Pugacheva, E. M., Loukinov, D. I., Goodwin, G. H., Delgado, D., Filippova, G. N., Leon, J., Morse, H. C., 3rd, Neiman, P. E. and Lobanenkova, V. V. (2001) Functional phosphorylation sites in the C-

- terminal region of the multivalent multifunctional transcriptional factor CTCF. *Mol. Cell Biol.* **21**, 2221-2234
- 35 Caiafa, P. and Zlatanova, J. (2009) CCCTC-binding factor meets poly(ADP-ribose) polymerase-1. *physiology. Cell. Physiol.*
- 36 Xiao, T., Wallace, J. and Felsenfeld, G. (2011) Specific sites in the C terminus of CTCF interact with the SA2 subunit of the cohesin complex and are required for cohesin-dependent insulation activity. *Mol. Cell Biol.* **31**, 2174-2183
- 37 Kanduri, C., Pant, V., Loukinov, D., Pugacheva, E., Qi, C. F., Wolffe, A., Ohlsson, R. and Lobanenko, V. V. (2000) Functional association of CTCF with the insulator upstream of the H19 gene is parent of origin-specific and methylation-sensitive. *Curr Biol.* **10**, 853-856
- 38 Zhang, R., Burke, L. J., Rasko, J. E., Lobanenko, V. and Renkawitz, R. (2004) Dynamic association of the mammalian insulator protein CTCF with centrosomes and the midbody. *Exp. Cell Res.* **294**, 86-93
- 39 Yusufzai, T. M., Tagami, H., Nakatani, Y. and Felsenfeld, G. (2004) CTCF tethers an insulator to subnuclear sites, suggesting shared insulator mechanisms across species. *Mol. Cell.* **13**, 291-298
- 40 Dunn, K. L., Zhao, H. and Davie, J. R. (2003) The insulator binding protein CTCF associates with the nuclear matrix. *Exp. Cell Res.* **288**, 218-223
- 41 Docquier, F., Kita, G. X., Farrar, D., Jat, P., O'Hare, M., Chernukhin, I., Gretton, S., Mandal, A., Alldridge, L. and Klenova, E. (2009) Decreased poly(ADP-ribosylation) of CTCF, a transcription factor, is associated with breast cancer phenotype and cell proliferation. *Clin. Cancer Res.* **15**, 5762-5771
- 42 Wan LB, Pan H, Hannenhalli S, Cheng Y, Ma J, Fedoriw A, Lobanenko V, Latham KE, Schultz RM, Bartolomei MS. (2008) Maternal depletion of CTCF reveals multiple functions during oocyte and preimplantation embryo development. *Development.* **135**, 2729-38.
- 43 Wang ZQ, Auer B, Stingl L, Berghammer H, Haidacher D, Schweiger M, Wagner EF (1995). Mice lacking ADPRT and poly(ADP-ribosylation) develop normally but are susceptible to skin disease. *Genes Dev.* **9**, 509-20
- 44 Kanai, M., Hanashiro, K., Kim, S. H., Hanai, S., Boulares, A. H., Miwa, M. and Fukasawa, K. (2007) Inhibition of Crm1-p53 interaction and nuclear export of p53 by poly(ADP-ribosylation). *Nat. Cell Biol.* **9**, 1175-1183
- 45 Zerfaoui, M., Errami, Y., Naura, A. S., Suzuki, Y., Kim, H., Ju, J., Liu, T., Hans, C. P., Kim, J. G., Abd Elmageed, Z. Y., Koochekpour, S., Catling, A. and Boulares, A. H. (2010) Poly(ADP-ribose) polymerase-1 is a determining factor in Crm1-mediated nuclear export and retention of p65 NF-kappa B upon TLR4 stimulation. *J Immunol.* **185**, 1894-1902
- 46 Di Paola S, M. M., Di Tullio G, Buccione R, Di Girolamo M. (2012.) PARP16/ARTD15 Is a Novel Endoplasmic-Reticulum-Associated Mono-ADP-Ribosyltransferase That Interacts with, and Modifies Karyopherin-β1. *PLoS One.* **7**, e37352
- 47 Macaluso, M., Caracciolo, V., Rizzo, V., Sun, A., Montanari, M., Russo, G., Bellipanni, G., Khalili, K. and Giordano, A. (2012) Integrating role of T antigen, Rb2/p130, CTCF and BORIS in mediating non-canonical endoplasmic reticulum-dependent death pathways triggered by chronic ER stress in mouse medulloblastoma. *Cell cycle (Georgetown, Tex.)* **11**, 1841-1850
- 48 Caiafa, P. and Zampieri, M. (2005) DNA methylation and chromatin structure: the puzzling CpG islands. *J.Cell. Biochem.* **94**, 257-265

49 Su CH, Shann YJ, Hsu MT. (2009) p53 chromatin epigenetic domain organization and p53 transcription. *Mol. Cell. Biol.* **29**, 93-103.

Accepted Manuscript

THIS IS NOT THE VERSION OF RECORD - see doi:10.1042/BJ20121429

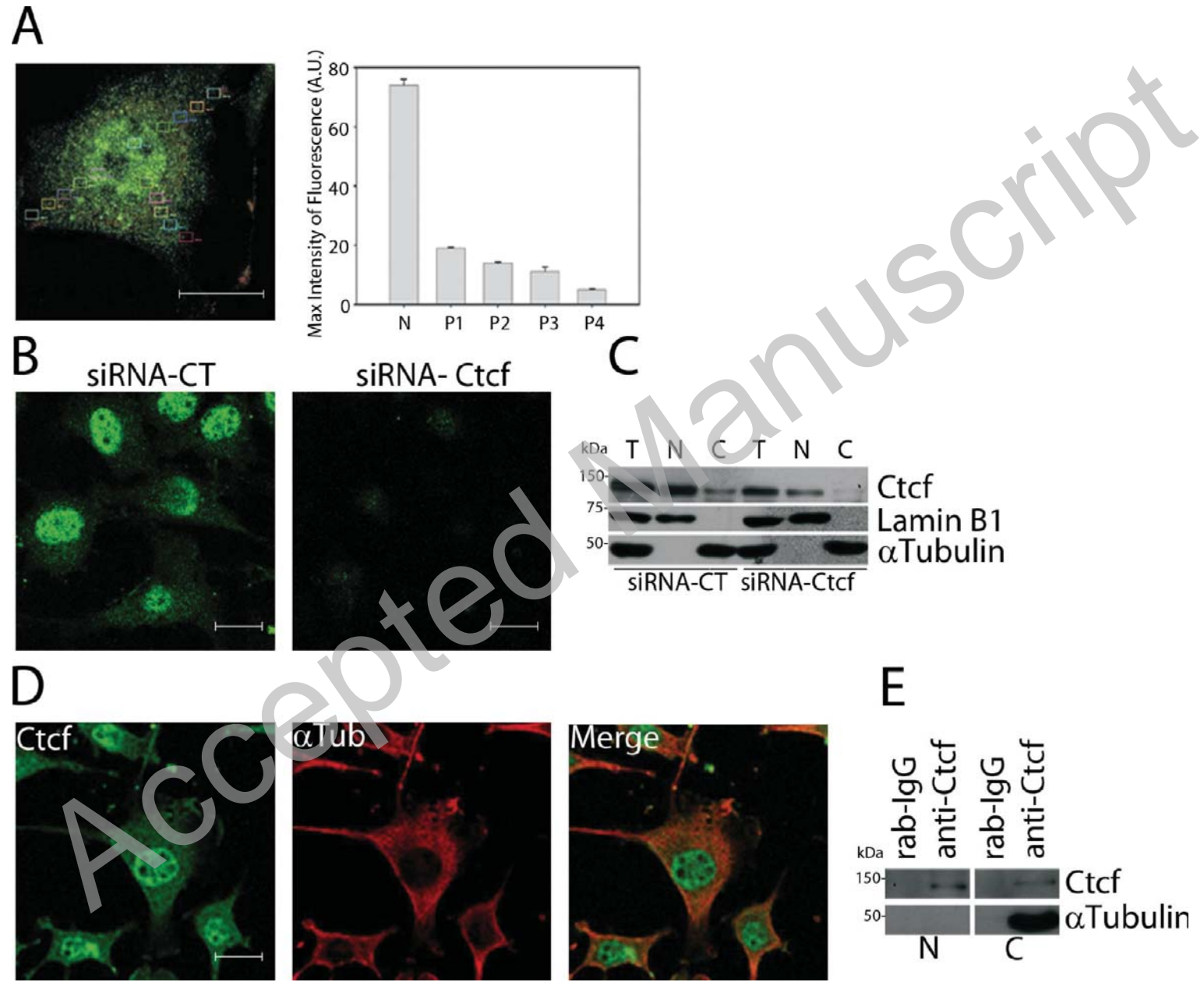
FIGURES LEGENDS

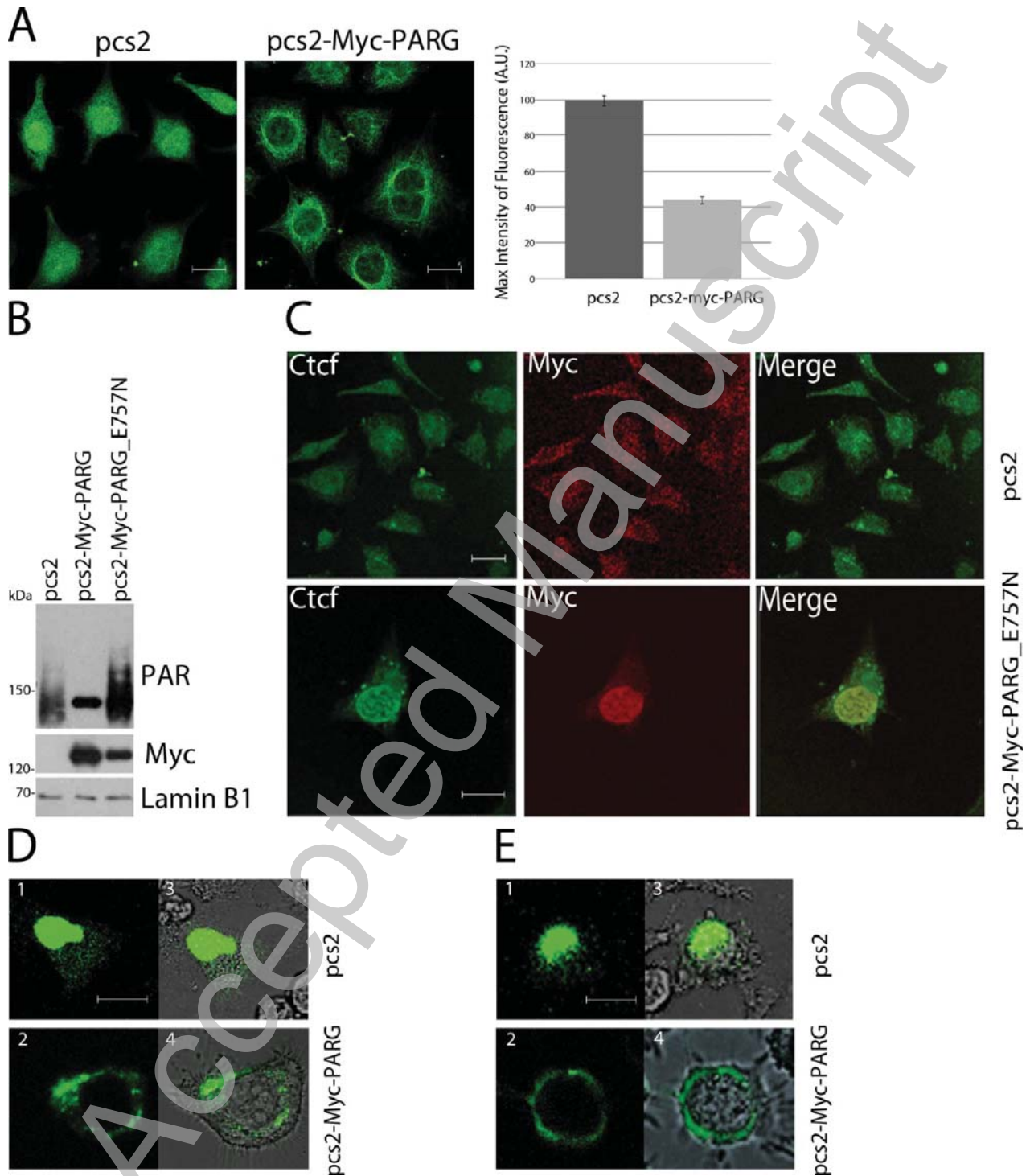
Figure 1. **Analysis of cellular localization of Ctcf in L929 mouse fibroblasts.** **A.** The CLSM of L929 cells incubated with anti Ctcf antibodies (green). Coloured squares represent areas at different distance from the nucleus used for the quantitative analysis of fluorescence. Right panel shows the histogram representing the fluorescence evaluated in the nucleus (N) and in cytosol at different distance from the nucleus (P1, P2, P3 and P4) (A.U. arbitrary units). Data are reported as mean \pm S.E. **B.** CLSM of control (siRNA-CT) and Ctcf silenced (siRNA-Ctcf) L929 cells incubated with anti Ctcf antibodies. **C.** Western blot analysis of nuclear and cytosolic fractions isolated from control and Ctcf silenced L929 cells performed with anti Ctcf antibodies (T: total cell extract; N: nuclear extract and C: cytosolic extract). Lamin B1 and α Tubulin were used as control for purity of nuclear and cytosolic fraction respectively. **D.** CLSM of L929 cells incubated with anti Ctcf (green) and anti α Tubulin antibodies (red), right panel represents the merge image. **E.** Ctcf immunoprecipitation experiments carried out using L929 nuclear (N) and cytosolic (C) fractions with the anti Ctcf and anti α Tubulin antibodies. Scale bars 20 μ m.

Figure 2. **Role of PARs in Ctcf nuclear re-localization.** **A.** CLSM of L929 cells overexpressing pcs2-Myc-PARG vector and the corresponding control (pcs2) using the anti Ctcf antibodies. The histogram presenting Ctcf fluorescence in PARG overexpressing L929 cells relative to the fluorescence in control cells, is shown on the right. Data are reported as mean \pm S.E. **B.** Western blot analysis of L929 cells overexpressing PARG, pcs2-Myc-PARG_E757N and the empty vector pcs2, after 72 hours with puromycin. Analyses were performed with the anti PAR, anti Myc and Lamin B1 (control) antibodies. **C.** CLSM of L929 cells overexpressing pcs2 and pcs2-Myc-PARG_E757N incubated with the anti Ctcf (green) and anti Myc (red) antibodies, right panel is the merged image. **D.** CLSM of L929 cells co-overexpressing pcs2 / EGFP-CTCF wild type (1, 3) and pcs2-Myc-PARG / EGFP-CTCF wild type (2, 4) vectors. In 3 and 4 the same images are displayed in transmitted light. **E.** CLSM of L929 cells co-overexpressing pcs2 / EGFP-CTCF mutant deficient for PARylation (1, 3) and pcs2-Myc-PARG / EGFP-CTCF mutant (2, 4) vectors. In 3 and 4 the same images are displayed in the transmitted light. Scale bars 20 μ m.

Figure 3. **Ctcf interactions at the nuclear periphery.** **A.** CLSM of L929 cells overexpressing pcs2-Myc-PARG and the corresponding empty vector pcs2 using the anti Ctcf (green) and Lamin B1 (red) antibodies. Merged immunofluorescence images are shown on the right. **B.** Co-immunoprecipitation of Ctcf in L929 lysates immunoblotted using anti NPC, anti Ctcf and anti PAR antibodies. Normal IgGs were used as negative control. Scale bars 20 μ m.

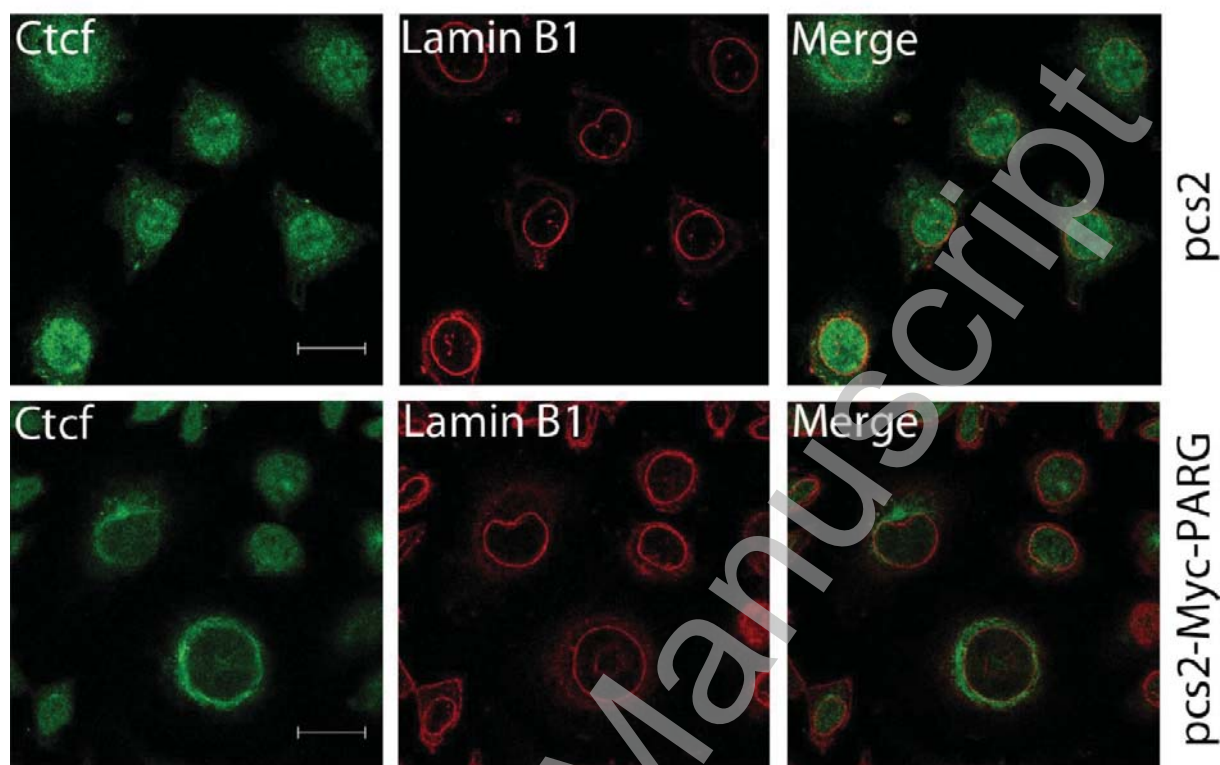
Figure 4. **DNA rearrangement dependent on PAR depletion.** **A.** Nuclear DNA staining with TO-PRO-3 of pcs2 and pcs2-Myc-PARG overexpressing cells. The inserts show enlarged details of the respective images. On the right there is a graph showing fluorescence intensity as a function of the distance (measured in micrometers) of multiple peaks recovered in different nuclear areas of cells randomly chosen. **B.** CLSM of L929 cells overexpressing pcs2-Myc-PARG and the relative empty vector pcs2 using anti 2me-H3K4, anti 5-MeCyt and anti 3me-H3K9. **C.** CLSM of Ctcf silenced L929 and the relative control cells incubated with both anti Ctcf and anti 2me-H3K4, anti 5-MeCyt and anti 3me-H3K9 antibodies. Scale bars 20 μ m.



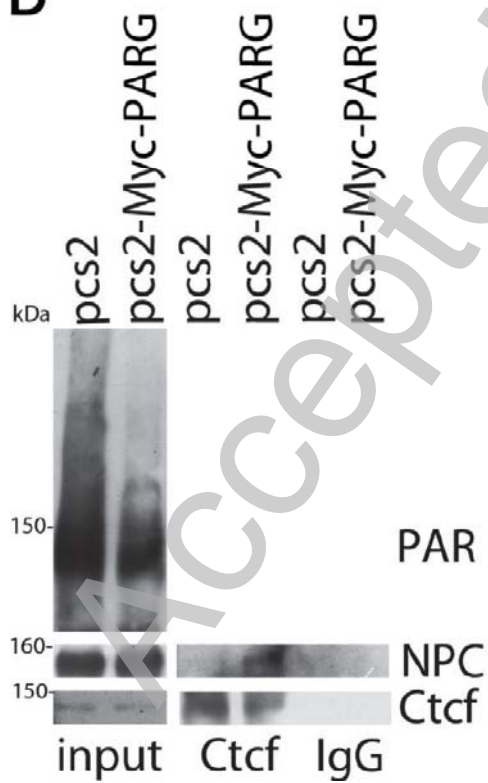


THIS IS NOT THE VERSION OF RECORD - see doi:10.1042/BJ20121429

A



B



THIS IS NOT THE VERSION OF RECORD - see doi:10.1042/BJ20121429

